JOURNAL OF BACTERIOLOGY, Aug. 2007, p. 5482–5494 Vol. 189, No. 15
0021-9193/07/$08.00+0 doi:10.1128/JB.00647-07

Cysteine Scanning Mutagenesis and Topological Mapping of the *Escherichia coli* Twin-Arginine Translocase TatC Component▽

Claire Punginelli,[1] Bárbara Maldonado,[1,2] Sabine Grahl,[1] Rachael Jack,[1,2]† Meriem Alami,[3] Juliane Schröder,[1] Ben C. Berks,[3] and Tracy Palmer[1,2]*

Department of Molecular Microbiology, John Innes Centre, Norwich NR4 7UH, United Kingdom[1]; School of Biological Sciences, University of East Anglia, Norwich NR4 7TJ, United Kingdom[2]; and Department of Biochemistry, University of Oxford, South Parks Road, Oxford OX1 3QU, United Kingdom[3]

Received 25 April 2007/Accepted 22 May 2007

The TatC protein is an essential component of the *Escherichia coli* twin-arginine (Tat) protein translocation pathway. It is a polytopic membrane protein that forms a complex with TatB, together acting as the receptor for Tat substrates. In this study we have constructed 57 individual cysteine substitutions throughout the protein. Each of the substitutions resulted in a TatC protein that was competent to support Tat-dependent protein translocation. Accessibility studies with membrane-permeant and -impermeant thiol-reactive reagents demonstrated that TatC has six transmembrane helices, rather than the four suggested by a previous study (K. Gouffi, C.-L. Santini, and L.-F. Wu, FEBS Lett. 525:65–70, 2002). Disulfide cross-linking experiments with TatC proteins containing single cysteine residues showed that each transmembrane domain of TatC was able to interact with the same domain from a neighboring TatC protein. Surprisingly, only three of these cysteine variants retained the ability to cross-link at low temperatures. These results are consistent with the likelihood that most of the disulfide cross-links are between TatC proteins in separate TatBC complexes, suggesting that TatC is located on the periphery of the complex.

Proteins are transported across the cytoplasmic membranes of bacteria and the thylakoid membranes of plants by one of two general protein transport pathways. The Sec pathway translocates linear polypeptides by a threading mechanism, powered by a combination of the transmembrane proton gradient and the ATPase SecA (27). By contrast, the Tat system transports folded proteins, driven solely by the energy of the proton motive force. Proteins are targeted to either the Sec or Tat pathway by means of N-terminal signal peptides. While there is no consensus amino acid motif present in signal peptides targeting to the Sec pathway, Tat signal peptides almost always contain a signature pair of consecutive arginines that are critical for efficient export by the Tat pathway (reviewed in references 5 and 31).

In the model prokaryote *Escherichia coli*, four genes encode components of the Tat machinery (6, 37, 38, 44). TatA, TatB, and TatC are the major subunits of the Tat translocon, while *tatE* encodes a poorly expressed ortholog of TatA (20). The sequences of the TatA and TatB proteins are related, each possessing a single transmembrane domain at the N terminus with an N_{out}-C_{in} topology (12, 17, 23). Despite sharing sequence similarity, they have distinct functions in protein transport and cannot substitute for one another (38). The TatC protein is the largest and most hydrophobic Tat component. Bioinformatic analysis suggests that it has six membrane-spanning domains (6, 15). An early topological study using compartment-sensitive marker fusions questioned the topology prediction because it indicated that the protein had only four transmembrane domains and a large periplasmic loop encompassing predicted helices 4 and 5 (18) (see Fig. 1). The topology of TatC was subsequently revisited using similar fusion protein technology giving results that were in broad agreement with the six-transmembrane-domain model (4, 21).

Biochemical studies have identified two types of high-molecular-weight complexes containing Tat components in *E. coli* membranes. A heterogeneous complex of TatA has been purified from membranes of strains either overexpressing *tatA* alone or all three essential Tat components (17, 35, 39). Analysis of this complex by negative stain electron microscopy shows that it exists as ring-like structures, which suggests that it forms the protein-conducting channel (17). A separate complex, comprising equimolar amounts of TatB and TatC, has been isolated from *E. coli* membranes, and a similar complex has also been identified in the membranes of plant thylakoids (7, 10, 13, 29). A small and variable amount of TatA is found associated with this complex when all three proteins are produced at elevated levels but not at native levels (30). The size of the TatBC complex varies between 370 kDa and about 650 kDa depending on the detergent used for its extraction, but given the masses of its constituent protomers (18.4 kDa for TatB and 28.9 kDa for TatC), it clearly must be a higher-order multimer. In vitro cross-linking studies for both thylakoid and bacterial systems have shown that substrates interact initially with the TatBC complex (1, 10). Using site-specific cross-linking analysis, TatB was shown to interact with the hydrophobic core region of the signal peptide, while TatC contacted the signal peptide close to the twin arginines, strongly suggesting that it is primarily responsible for recognition of the consensus motif (1, 16).

* Corresponding author. Mailing address: Department of Molecular Microbiology, John Innes Centre, Colney Lane, Norwich NR4 7UH, United Kingdom. Fax: (44) (1603) 450778. E-mail: tracy.palmer@bbsrc.ac.uk.

† Present address: Department of Molecular Microbiology, Karakorum International University, Gilgit, Northern Areas, Pakistan.

▽ Published ahead of print on 1 June 2007.

Low-resolution negative stain electron microscopy studies of TatBC complexes, containing small amounts of TatA derived from *E. coli* membranes overexpressing native Tat components or those of *Salmonella enterica* serovar Typhimurium or *Agrobacterium tumefaciens* revealed the presence of oval-shaped particles. The particles were lobed, with five, six, or seven lobes depending in part on the origin of the Tat proteins. Each lobe was estimated to comprise seven or eight transmembrane helices and therefore might correspond to a single TatBC unit (33). Blue native polyacrylamide gel electrophoresis (PAGE) analysis indicates that the TatBC complex minimally contains six or seven copies of each subunit (34). A recent cysteine scanning mutagenesis and disulfide cross-linking study has shown that within the TatBC complex, TatB is arranged as a higher-order homo-oligomer, probably at least a tetramer (23). Since TatB and TatC have a 1:1 stoichiometry (7), these observations indicate that TatC should also be organized as a multimer and that to accommodate the constraints imposed by the homo-oligomerization of TatB, TatC should be present on the outside of the complex (23). In this study we have constructed a bank of individual cysteine substitutions in the *E. coli* TatC protein and used these to investigate the topological organization and oligomeric arrangement of the protein. Our results confirm the six-transmembrane-helix model of TatC. Moreover, they show that TatC is organized as at least a dimer and that each of the six transmembrane helices make self-contacts, consistent with the idea that TatC is located on the periphery of the TatBC complex.

MATERIALS AND METHODS

Bacterial strains, plasmids, and growth conditions. Trimethylamine-*N*-oxide (TMAO) reductase activity and cysteine labeling and cross-linking experiments were performed in *E. coli* strain DADE-P [same as strain MC4100 (9) but with Δ*tatABCD* Δ*tatE pcnB1 zad-981*::Tn*10d* (Km^r); 23]. For assessment of in vivo disulfide bond formation, *E. coli* strain LM107 was used [F$^-$ *araD139* Δ(*araABC-leu*)*7679 galU galK* Δ(*lac*)*X74 rpsL thi phoR zih-12*::Tn*10 dsbA*::Cm (28)]. Plasmids pUNITATCC4 and pUNITATCC4H have been described previously (23). Each plasmid harbors *tatA*, *tatB*, and the cysteine codonless derivative of *tatC* in pQE60 (QIAGEN). Convenient restriction sites have been engineered between *tatB* and *tatC*, allowing easy replacement of each individual gene. In addition, plasmid pUNITATCC4H supplies TatC with a C-terminal hexahistidine tag ($TatC_{His}$).

A plasmid, pUNITATC, that contains the *tatC* gene in pBluescript was constructed following amplification of the *tatC* gene with primers UNIC1 (5′-GCGCGAATTCCTTAAGCATGTCTGTAGAAGATACT-3′) and UNIC2 (5′-GCGCGGATCCTTATTCTTCAGTTTTTTCGCTTTCT-3′; restriction sites underlined), digestion with EcoRI and BamHI, and cloning into pBluescript that had been previously digested with the same enzymes. Site-specific cysteine mutations were initially introduced into the *tatC* gene in plasmid pUNITATC using the QuikChange method. Each mutant *tatC* allele was subsequently excised from pUNITATC by digestion with AflII and BamHI and cloned into pUNITATCC4 that had been similarly digested. For cysteine labeling experiments, *tatC* alleles were cloned into pUNITATCC4H. This was achieved by amplification of the mutated *tatC* genes in pUNITATC using primers UNIC1 and TATCH2 (13), digestion with AflII and BglII, and cloning into pUNITATCC4H that had been similarly digested. The individual cysteine substitutions used in this work are shown in Table 1.

All clones obtained from PCR-amplified DNA were sequenced to ensure that no undesired mutations had been introduced. The primer sequences for introduction of site-specific mutations are available on request.

During all genetic manipulations and for cysteine cross-linking experiments, *E. coli* strains were grown aerobically in Luria-Bertani (LB) medium (36). Strains were normally grown at 37°C unless otherwise stated. Concentrations of antibiotics were as described previously (37). The growth phenotypes of mutants with TMAO as the sole respiratory electron acceptor were determined on M9 minimal medium agar plates (36) supplemented with 0.5% glycerol and 0.4% TMAO and incubated in a gas jar under a hydrogen/carbon dioxide atmosphere. The sodium dodecyl sulfate (SDS) resistance phenotype of mutants was tested on LB agar plates containing 2% SDS (8). For TMAO reductase assays, cells were cultured in modified Cohen and Rickenberg medium (11) supplemented with 0.2% (wt/vol) glucose and 0.4% (wt/vol) TMAO. Subcellular fractions for TMAO reductase assays were prepared from small (30-ml) cultures using a cold osmotic shock protocol (41), and TMAO:benzyl viologen oxidoreductase activity was measured as described previously (40). Spheroplasts for sulfhydryl labeling experiments were prepared from 500-ml cultures using the lysozyme-EDTA method (37). For strains harboring plasmids producing the TatC G144C or S148C variant, 5 mM dithiothreitol (DTT) was included in the incubation buffer during spheroplast preparation.

Sulfhydryl labeling of cysteine residues. Labeling experiments were carried out on spheroplasts prepared from strains expressing *tatA*, *tatB*, and single cysteine variants of $tatC_{His}$. Three independent reactions were carried out for each sample, one where spheroplasts were treated with the membrane-permeable, sulfhydryl-reactive compound, N^{α}-(3-maleimidylproprionyl)biocytin (MPB; Molecular Probes) the second where spheroplasts were pretreated with the membrane-impermeable blocking reagent 4-acetamido-4′-maleimidylstilbene-2,2′-disulfonic acid (AMS; Molecular Probes) prior to treatment with MPB, and the third, which was an untreated control sample.

For each reaction, intact spheroplasts (400 μg of protein) were resuspended in 500 μl of 50 mM Tris-HCl (pH 7.6) and 0.5 M sucrose. For treatment with AMS, 0.5 mM AMS (in water) was added to the sample, which was incubated for 20 min at room temperature with gentle shaking. Excess AMS was removed by gentle centrifugation, and the spheroplasts were resuspended in 500 μl of 50 mM Tris-HCl (pH 7.6) and 0.5 M sucrose. For reaction with MPB, 1 mM MPB (in dimethyl formamide) was added to the spheroplast suspension, which was incubated for 20 min at room temperature with gentle shaking. The control sample (spheroplast suspension alone) was also incubated for 20 min at room temperature with shaking. After the incubation, all samples were quenched by the addition of 500 μl of 50 mM Tris-HCl (pH 7.6), 0.5 M sucrose, and 100 mM β-mercaptoethanol and incubated for 15 min at room temperature with gentle shaking. Spheroplasts were then disrupted by sonication on ice for five 15-s bursts (10-micron amplitude) with 15-s intervals. Cell debris was removed by centrifugation at 10,000 × *g* at 4°C for 5 min, and membrane proteins were recovered by ultracentrifugation at 278,000 × *g* for 30 min. The pellet was resuspended in 100 μl of 50 mM Tris-HCl, pH 6.8, and samples were denatured by the addition of 1% SDS and incubated at 37°C for 15 min prior to immunoprecipitation.

Immunoprecipitation of TatC protein. Protein A Sepharose CL-4B (Amersham) was resuspended to 10 mg/ml in buffer A [25 mM Tris-HCl, pH 6.8, 0.9% (wt/vol) NaCl, 1% Triton X-100, 5 mM EDTA, pH 8.0]. Twenty microliters of anti-TatC antibody was added per ml of protein A Sepharose, and the samples were incubated for 3 h at 4°C with gentle shaking to allow binding of the antibody to protein A. After incubation, unbound antibodies were removed by centrifugation at room temperature at 10,000 × *g*, and the Sepharose beads were washed twice with buffer A. The pelleted beads were resuspended to 10 mg/ml in buffer A, and 10 mg of antibody-loaded protein A Sepharose was added to each denatured membrane protein fraction. Samples were incubated at 4°C overnight with gentle shaking to allow binding of the antigen to the immunoglobulins. The Sepharose beads were then pelleted by centrifugation at 10,000 × *g* for 2 min to remove unbound proteins. The pellet was washed twice with 1 ml of buffer A, and the beads were resuspended in 1 ml of 25 mM Tris-HCl, pH 6.8, and again pelleted by centrifugation at 10,000 × *g* for 2 min. The pellet was finally resuspended in 25 μl standard SDS loading buffer (50 mM Tris-HCl, pH 6.8, 2% SDS, 10% glycerol, 0.1% bromophenol blue, 1% β-mercaptoethanol [final concentrations given]) and denatured by incubation at 56°C for 20 min prior to SDS-PAGE.

Other protein methods. Membrane preparation and disulfide cross-linking were carried out essentially by the methods of Lee et al. (23) with the exception that oxidant-induced cross-linking was carried out for 1 hour at either 20°C or on ice as indicated below. The following modification was included for the reduction of spontaneous cross-linked samples. Membrane fractions in buffer 1 (50 mM Tris-HCl, pH 7.5, 5 mM $MgCl_2$, 10% (vol/vol) glycerol; 50-μl final volume) were treated with 1 μl of 0.5 M DTT on ice for 1 h. Membranes were washed twice with buffer 1 to remove excess DTT and resuspended in buffer 1. Helical wheels were drawn using the "helical wheel" program of the Wisconsin Package, version 10.2 using the default setting of 3.6 amino acid residues per turn.

Polyclonal anti-TatC antibodies were raised in rabbits using the peptide NH_2-CGKGRNREEENDAEAESEKTEE-COOH, by Affiniti (BIOMOL International, Exeter, United Kingdom). Anti-tetra-His tag antibody (mouse) was obtained from QIAGEN, SDS-PAGE and immunoblotting were carried out as

TABLE 1. TatC cysteine substitutions used during this study

Plasmid	Relevant characteristic(s)	Mutation	Reference
pUNITAT2	TatA, TatB, and TatC with C-terminal hexa-His tag in pQE60		29
pUNITATCC4H	Cysteine-less TatABC in pQE60. TatC supplied with C-terminal hexa-His tag	TatC C23A (TGC→GCC), C33A (TGT→GCT), C179A (TGC→GCC), C224A (TGT→GCT)	23
Plasmids with TatB cysteine mutations in pUNITATCC4H			
pUNIHCPC9	L9C	L9C (CTT→TGT)	This work
pUNIHCPC144	G144C	G144C (GGG→TGT)	This work
pUNIHCPC148	S148C	S148C (TCC→TGC)	This work
pUNIHCPC183	I183C	I183C (ATT→TGT)	This work
pUNIHCPC186	P186C	P186C (CCA→TGT)	This work
pUNIHCPC191	K191C	K191C (AAA→TGT)	This work
pUNITATCC4	Cysteine-less TatABC in pQE60	TatC C23A (TGC→GCC), C33A (TGT→GCT), C179A (TGC→GCC), C224A (TGT→GCT)	23
Plasmids with TatC cysteine mutations in pUNITATCC4			
Cysteine substitutions in TMH1[a]			
pUNIBMC20	L20C	L20C (CTG→TGT)	This work
pUNIBMC21	L21C	L21C (CTG→TGT)	This work
pUNIBMC22	N22C	N22C (AAC→TGT)	This work
pUNIBMC23	C23C	C23C (TGC→TGT)	This work
pUNIBMC24	I24C	I24C (ATT→TGT)	This work
pUNIBMC25	I25C	I25C (ATC→TGT)	This work
pUNIBMC26	A26C	A26C (GCG→TGT)	This work
pUNIBMC27	V27C	V2YC (GTG→TGT)	This work
pUNICPC28	I28C	I28C (ATC→TGC)	This work
pUNICPC29	V29C	V29C (GTG→TGT)	This work
pUNICPC30	I30C	I30C (ATA→TGC)	This work
pUNICPC31	F31C	F31C (TTC→TGC)	This work
pUNICPC32	L32C	L32C (CTG→TGT)	This work
pUNICPC33	C33C	A33C (GCG→TGT)	This work
pUNIBMC34	L34C	L34C (CTG→TGT)	This work
pUNIBMC35	V35C	V35C (GTC→TGT)	This work
pUNIBMC36	Y36C	Y36C (TAT→TGT)	This work
pUNIBMC37	F37C	F37C (TTC→TGT)	This work
pUNIBMC38	A38C	A38C (GCC→TGT)	This work
pUNIBMC39	N39C	N39C (AAT→TGT)	This work
pUNIBMC40	D40C	D40C (GAC→TGT)	This work
Cysteine substitutions in TMH2			
pUNICPC81	I81C	I81C (ATT→TGT)	This work
pUNICPC82	L82C	L82C (CTG→TGC)	This work
pUNICPC83	S83C	S83C (TCA→TGC)	This work
pUNICPC84	A84C	A84C (GCG→TGC)	This work
pUNICPC85	P85C	P85C (CCG→TGC)	This work
pUNICPC86	V86C	V86C (GTG→TGC)	This work
Cysteine substitutions in TMH3			
pUNICPC124	F124C	F124C (TTC→TGC)	This work
pUNICPC125	A125C	A125C (GCC→TGC)	This work
pUNICPC126	Y126C	Y126C (TAC→TGC)	This work
pUNICPC127	F127C	F127C (TTT→TGT)	This work
pUNICPC128	V128C	V128C (GTG→TGC)	This work
pUNICPC129	V129C	V129C (GTC→TGC)	This work
Cysteine substitutions in TMH4			
pUNICPC166	G166C	G166C (GGT→TGT)	This work
pUNICPC167	V167C	V167C (GTC→TGC)	This work
pUNICPC168	S168C	S168C (TCC→TGC)	This work
pUNICPC169	F169C	F169C (TTT→TGT)	This work
pUNICPC170	E170C	E170C (GAA→TGC)	This work
pUNICPC171	V171C	V171C (GTG→TGC)	This work
Cysteine substitutions in TMH5			
pUNICPC200	A200C	A200C (GCA→TGC)	This work
pUNICPC201	F201C	F201C (TTC→TGC)	This work

Continued on following page

TABLE 1—*Continued*

Plasmid	Relevant characteristic(s)	Mutation	Reference
pUNICPC202	V202C	V202C (GTT→TGT)	This work
pUNICPC203	V203C	V203C (GTC→TGC)	This work
pUNICPC204	G204C	G204C (GGG→TGC)	This work
pUNICPC205	M205C	M205C (ATG→TGC)	This work
Cysteine substitutions in TMH6			
pUNICPC227	E227C	E227C (GAA→TGC)	This work
pUNICPC228	I228C	I228C (ATC→TGC)	This work
pUNICPC229	G229C	G229C (GGT→TGT)	This work
pUNICPC230	V230C	V230C (GTC→TGC)	This work
pUNICPC231	F231C	F231C (TTC→TGC)	This work
pUNICPC232	F232C	F232C (TTC→TGC)	This work

[a] TMH1, transmembrane helix one.

described previously (22, 43), and immunoreactive bands were visualized with the ECL detection system (Amersham Biosciences). MPB-labeled protein was detected using streptavidin-horseradish peroxidase (HRP) (Amersham Biosciences). Protein concentrations were estimated by the method of Lowry et al. (25). Spheroplast intactness was assayed by monitoring the activity of the cytoplasmic marker enzyme glucose-6-phosphate dehydrogenase (3).

RESULTS

Topological analysis of the TatC protein. Topological fusion studies using compartment-specific marker proteins have given conflicting results about the number of transmembrane segments in the *E. coli* TatC protein. In silico predictions suggest that in general, TatC proteins (with the exception of the much larger fused dimeric TatC proteins of some members of the domain Archaea) possess six transmembrane spans. An initial fusion study suggested that TatC had only four transmembrane domains (18), while two later studies using similar fusion technology suggested that the protein had six transmembrane domains (4, 21). A general criticism of fusion studies is that they can influence the topology of the protein to which they are fused. Moreover, they usually inactivate the protein under study. We therefore sought to investigate the presence or absence of the controversial transmembrane domains four and five (Fig. 1)

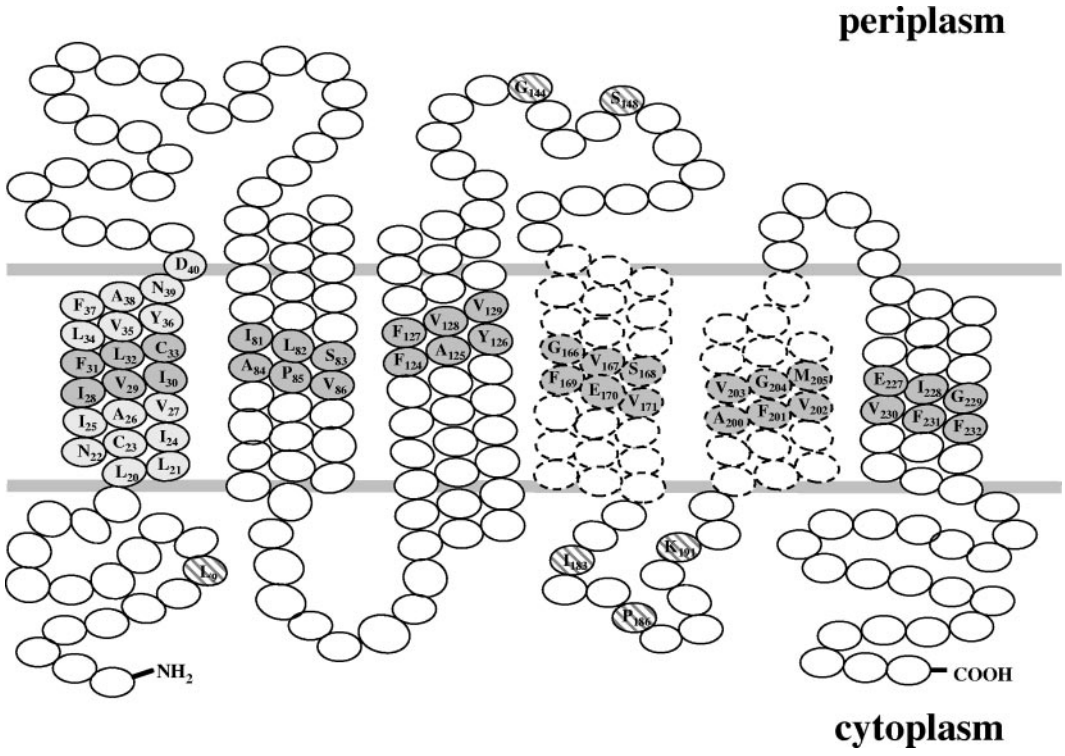

FIG. 1. Positions of the single cysteine substitutions in TatC that were constructed in this study. Residues that were substituted to cysteine for topological labeling studies are shown in hatched ovals, while those located towards the center of each predicted transmembrane α-helix that were substituted to cysteine for the initial disulfide cross-linking analysis are represented as solid medium-gray ovals. Further residues in transmembrane helix one that were mutated to cysteine are depicted as solid light-gray ovals. Transmembrane helices four and five are shown in broken lines, since a study by Gouffi et al. (18) questioned their existence.

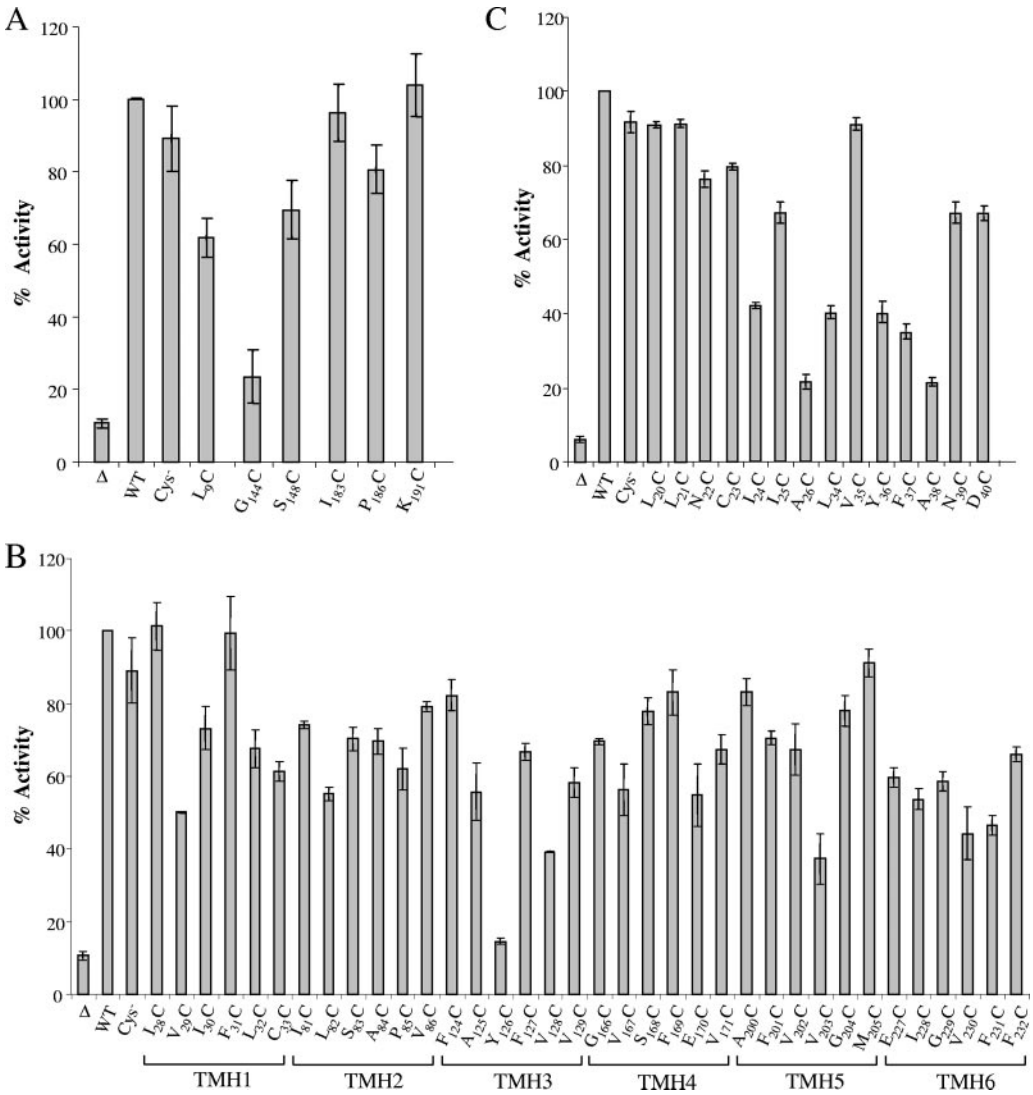

FIG. 2. Periplasmic TMAO reductase activities of *E. coli tat* mutant strains producing TatA, TatB and cysteine-substituted TatC proteins that were used for sulfhydryl labeling (A) or disulfide cross-linking (B and C). Periplasmic TMAO reductase activities were measured from the Δ*tatABCD* Δ*tatE pcnB* derivative, DADE-P (Δ), or DADE-P carrying either pUNITAT2 (29) (wild type [WT]) and (A) pUNITATCC4H (Cys^-) or pUNITATCC4H encoding cysteine-substituted TatC proteins or (B and C) pUNITATCC4 (Cys^-) or pUNITATCC4 encoding cysteine-substituted TatC proteins. In each case, the amino acid position of the substitution is shown under each column. One hundred percent activity was taken to be that determined for *E. coli* strain DADE-P carrying pUNITAT1 and corresponds to an activity of typically 0.85 μmol benzyl viologen oxidized/min/mg protein. In panel B, the substitutions in transmembrane helix one (TMH1) to transmembrane helix six (TMH6) are shown. The error bars represent the standard errors of the means ($n = 3$ or 4).

by assessing the cellular location of the intervening loop region using the noninvasive technique of cysteine substitution and topological labeling.

The cysteine substitutions we constructed to probe the topology of TatC are shown in Fig. 1. We initially constructed control cysteine substitutions at residues L9 (the N terminus of TatC has an unequivocal cytoplasmic location [7]) and G144 (periplasmic location, directly preceding transmembrane domain four). To probe the topological organization of predicted transmembrane helices four and five, we constructed individual cysteine substitutions in the loop region between these two predicted transmembrane domains at positions I183, P186, and K191 (Fig. 1). Each of these substitutions was introduced into a plasmid-encoded $tatC_{His}$ gene in which all of the native cysteine codons had been replaced by alanine and that was also coexpressed with *tatA* and *tatB*. Plasmids were subsequently transformed into a strain lacking all Tat components and that carried the *pcnB1* mutation to limit plasmid copy number (24), and the activity of the plasmid-encoded Tat system was assessed by measurement of the periplasmic activity of the Tat substrate protein TMAO reductase.

As shown in Fig. 2A, a Tat system harboring a cysteineless derivative of $TatC_{His}$ shows more than 90% of the periplasmic TMAO reductase activity of a strain producing the His-tagged but otherwise native TatC. This is in agreement with our previous observations that none of the four native cysteine resi-

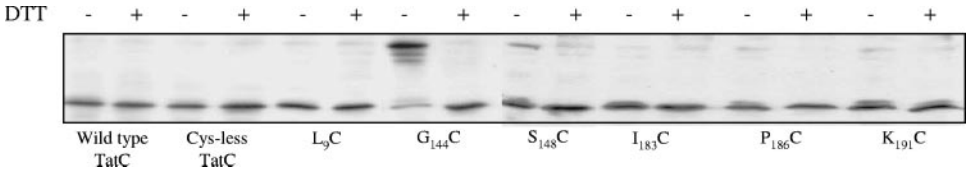

FIG. 3. TatC variant G144C forms a strong cross-linked dimer in untreated membranes. Western blot analysis of membranes isolated from the Δ*tatABCD* Δ*tatE pcnB* strain, *E. coli* strain DADE-P harboring plasmid producing TatA, TatB, and either wild-type $TatC_{His}$ (pUNITAT2), the $TatC_{His}$ cysteine-less derivative (pUNITATCC4H), or single cysteine substitutions as indicated. Samples were analyzed as isolated or were reduced by treatment with 10 mM DTT for 1 h (indicated by the symbols − and +, respectively, above each lane), and all samples were analyzed by SDS-PAGE under nonreducing conditions.

dues in TatC are essential for function (8, 23). A strain producing a TatC harboring the control substitution at L9C had periplasmic TMAO reductase activity that was about 60 to 70% of that of the wild type, indicating that the Tat system retained significant activity. By contrast, however, a strain producing TatC with the control G144C substitution showed much lower Tat activity (around 20% of that of the wild type). Since we wanted to ensure that our topological labeling studies were carried out on TatC proteins that were functional, we constructed an additional substitution of a residue in periplasmic loop 1, S148C. A strain producing a Tat system harboring this variant of TatC gave periplasmic TMAO reductase levels that were more than 70% of that of the wild type and therefore significantly more active than the G144C variant of TatC. The cysteine substitutions at I183, P186, and K191 designed to test the topology of TatC all gave TatC proteins that supported periplasmic TMAO reductase levels close to that of the wild type, indicating that none of our test substitutions significantly affected the activity and hence the topology of TatC.

Western blot analysis (Fig. 3) showed that each of the TatC variants was present in the membrane at a level similar to that of the wild-type protein. Interestingly, in the absence of a reducing agent, the TatC protein harboring the G144C substitution was found almost 100% in a disulfide-bonded dimer form. A small amount of the S148C TatC variant was also present as a dimer. These results suggest that the first periplasmic loop of TatC is found in close proximity (3 to 4 Å) to the same loop from a neighboring TatC and strongly suggests that TatC is arranged as at least a homodimer. It is also consistent with the fact that both of these residues are exposed at the periplasmic face of the membrane, where they would be accessible to the disulfide bond insertion machinery. However, we note that the level of disulfide-bonded dimer of the TatC G144C variant in whole cells of a *dsbA* strain was similar to that in the wild-type ($dsbA^+$) strain (data not shown).

In order to probe the location of the cysteine residue in each of the substituted TatC proteins, we used the following procedure. MPB is a membrane-permeable sulfhydryl-reactive compound that will react with cysteine residues regardless of their topological location (42). Thus, for intact spheroplasts (right-side-out membrane vesicles) it will react with cysteine residues that are located on the inside (cytoplasmic) or the outside (periplasmic location). Since it labels cysteine residues with a biotin moiety, labeling can be detected by probing with streptavidin-conjugated HRP during Western blotting. By contrast, AMS is a membrane-impermeable sulfhydryl-reactive compound that should react only with cysteine residues on the outer face of the cytoplasmic membrane (19). Thus, if spheroplasts are preincubated with an excess of AMS, cysteine residues that are exposed to the outside will react with this compound. Subsequent exposure to MPB will result in labeling of any remaining free cysteine residues. Therefore, cysteine residues that are inaccessible to AMS (on the inside of spheroplasts) will label with MPB, whereas those that are AMS accessible (i.e., on the outside) will be blocked from MPB labeling.

Patterns of MPB labeling of spheroplasts prepared from cells expressing a cysteineless variant of TatC along with single TatC variants L9C, G144C, and S148C are shown in Fig. 4A. For a TatC protein lacking cysteine residues, there is no labeling of the protein, showing that MPB labeling is dependent on the presence of cysteine. For TatC variant L9C, this residue was clearly labeled by MPB, regardless of whether spheroplasts containing this TatC derivative had been previously exposed to AMS. This pattern of labeling is consistent with a cytoplasmic location for this residue. It should be noted, however, that there was some reduction in the intensity of labeling with MPB after preexposure to the AMS block. This might be explained in part at least by the fact that there was some low-level breakage of spheroplasts during their preparation (data not shown). For TatC variant S148C, the labeling of the cysteine residue with MPB was totally blocked by prior exposure to AMS, confirming that this residue is exposed at the periplasmic side of the membrane. For TatC variant G144C, where we reduced the disulfide bond with DTT prior to the labeling experiments, MPB labeling of the cysteine was also blocked by preincubation with AMS, consistent with the exposure of this residue to the periplasmic face of the cytoplasmic membrane.

In order to test the location of the loop region between predicted transmembrane helices four and five, we next incubated spheroplasts harboring either the I183C, P186C, or K191C variants of TatC with one or both of the cysteine-reactive compounds. As shown in Fig. 4B, each of these cysteine residues was labeled when spheroplasts were incubated with MPB. Moreover, since labeling with MPB was not prevented by prior incubation of spheroplasts with the membrane-impermeable AMS reagent, these observations strongly suggest that each of these three residues are located at the cytoplasmic side of the membrane. Taken together, these results support in silico predictions (6, 15) and the more recent fusion studies (4, 21) which suggest that the *E. coli* TatC protein has six membrane-spanning domains.

Cysteine scanning mutagenesis of TatC. In order to probe the functions of residues within the transmembrane domains of

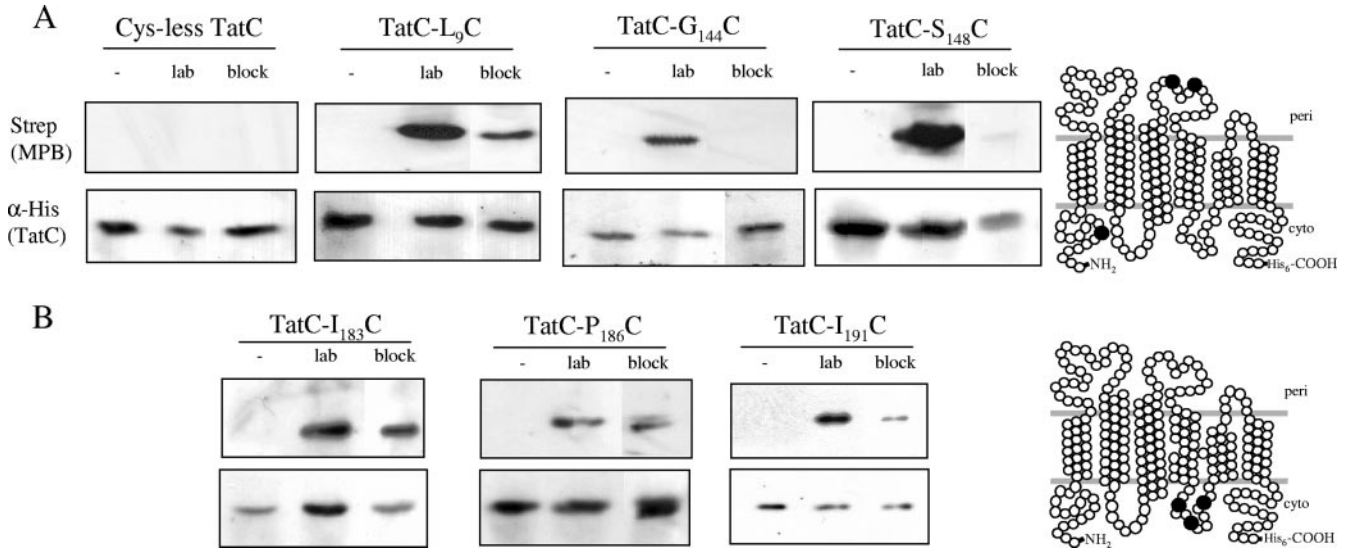

FIG. 4. Sulfhydryl labeling of spheroplasts overproducing TatA, TatB, and cysteine variants of TatC. Spheroplasts were incubated with buffer alone (−), with MPB (lab), or with AMS followed by MPB (block), as described in Materials and Methods. Spheroplasts were subsequently lysed, and membranes were isolated, dispersed with SDS, and immunoprecipitated with anti-TatC antisera. Samples were separated by SDS-PAGE (12.5% acrylamide) and electroblotted, and MPB-labeled protein was detected with a 1:5,000 dilution of streptavidin-HRP (Strep). The same blot was then stripped and reprobed with a 1:5000 dilution of anti-tetra-His (α-His) antibody (QIAGEN) to detect TatC protein. (A) Labeling reactions with control samples expressing a cysteine-less TatC variant and the single cysteine substitutions L9C (cytoplasmic location) and G144C and S148C (both periplasmic [peri] location). (B) Labeling reactions with TatC cysteine variants designed to probe the cellular location of the loop region between transmembrane helices four and five: I183C, P186C, and I191C. The positions of these residues on a cartoon of TatC are shown at the right-hand side of each panel (cytoplasmic [cyto] or periplasmic [peri] location).

TatC and as a prerequisite for disulfide mapping experiments, we constructed single cysteine substitutions in each of the six transmembrane domains of TatC. We initially selected six consecutive residues predicted to be towards the center of each transmembrane domain, as judged following alignment of multiple TatC sequences and then manual assignment of the positions of each of the transmembrane α-helices. These six residues were designed to cover almost two turns of a putative α-helix and were individually replaced by cysteine. The position of each of these substitutions is shown in Fig. 1. In transmembrane helix one, we constructed individual substitutions of I28, V29, I30, F31, L32, and C33 (which was originally alanine in our cysteineless derivative of TatC), in transmembrane helix two, we constructed substitutions of I81, L82, S83, A84, P85, and V86, in transmembrane helix three F124, A125, Y126, F127, V128, and V129, in transmembrane helix four G166, V167, S168, F169, E170, and V171, in transmembrane helix five A200, F201, V202, V203, G204, and M205, and in transmembrane helix six E227, I228, G229, V230, F231, and F232. Each of these substitutions was introduced into a plasmid-encoded *tatC* gene where all of the native cysteine codons had been replaced by alanine and that was also coexpressed with *tatA* and *tatB*. As above, in order to assess the functionality of Tat systems harboring TatC variants with each of these amino acid substitutions, plasmids were transformed into a strain lacking all Tat components and harboring the *pcnB1* allele, and the periplasmic activity of TMAO reductase was assessed.

As shown in Fig. 2B, strains with Tat systems harboring almost all of the cysteine substitutions showed periplasmic TMAO reductase activities that were greater than 50% of the activity of the wild type. The few exceptions to this were TatC V128C and TatC V203C substitutions (40 to 50% of wild-type activity) and TatC Y126C, which had very low activity. It should be noted that a Y126A substitution of TatC also similarly resulted in very low Tat activity (8), indicating that the presence of a tyrosine at this position, which is highly conserved among TatC proteins, is important for TatC function. We conclude that in general, cysteine substitution of transmembrane residues of TatC is well tolerated.

Disulfide mapping studies of TatC using single cysteine variants. Once we had constructed a bank of cysteine substitutions, we used them to map contact sites between TatC proteins. Disulfide mapping studies with TatB gave patterns of cross-linking that were consistent with the likelihood that TatB formed a homo-oligomeric ring located in the center of the TatBC complex (23). Given the probability that TatC is localized on the periphery, this in principle could give rise to two different types of cross-links. Cross-links could arise because the cysteines are located at contact sites between TatC monomers within the TatBC complex. Alternatively, cross-links could occur between TatC proteins that are present in different TatBC complexes. One way that these may be distinguished is to examine the effect of protein mobility on disulfide bridge formation. Cross-links that occur between different complexes are more susceptible to conditions that slow down the motion of complexes in the membrane, whereas cross-links within a complex are less so (32). One way that membrane fluidity can be altered is by lowering the temperature, which results in the reversible change of state from a disordered to an ordered array of fatty acyl chains (14, 26). Therefore, we undertook cross-linking experiments at room temperature and on

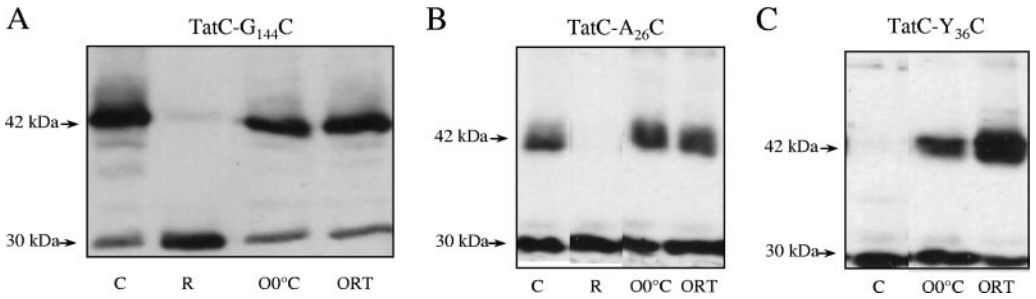

FIG. 5. The TatC G144C, A26C, and Y36C variants form disulfide cross-links when oxidized at room temperature or on ice. Membrane samples were prepared from the Δ*tatABCD* Δ*tatE pcnB* strain, DADE-P, coexpressing single cysteine-substituted TatC variants G144C (A), A26C (B), and Y36C (C) together with TatA and TatB from pUNITATCC4. For membranes harboring the TatC G144C or A26C substitution, a sample as prepared was retained (lanes marked C), and the remainder of the membranes were treated with DTT to reduce preformed dimer as described in Materials and Methods. Samples (100 μg membrane protein) were then subjected to oxidizing conditions (by the addition of copper phenanthroline) at either room temperature (ORT) or on ice (O0°C). A sample of the DTT-treated membranes are also shown (lanes marked R). For membranes harboring the TatC Y36C variant (which shows no disulfide-bonded dimer in the membrane as isolated), samples (100 μg membrane protein) were incubated for one hour with either buffer alone at room temperature (C) or oxidant at either room temperature (ORT) or on ice (O0°C). Samples (10 μg membrane protein) were resolved by SDS-PAGE (12.5% acrylamide), and TatC proteins were visualized by immunoblotting with anti-TatC antisera.

ice in order to distinguish cross-links likely to be formed between complexes from those formed within a single complex.

For cross-linking analysis, a plasmid encoding *tatA*, *tatB* and single cysteine-codon-substituted *tatC* was expressed in an otherwise *tat* mutant strain, membranes were prepared, and the ability of the single cysteine residue to form a disulfide bond with the identical residue in a neighboring TatC protein was assessed after exposure to oxidizing conditions. As shown in Fig. 3, we observed an almost 100% disulfide cross-linked dimeric form of TatC variant G144C in untreated membranes, demonstrating that this part of TatC is in close proximity with a neighbor. To test whether this cross-link was likely to be between TatC proteins in the same TatBC complex, we reduced the disulfide bond and then treated the sample with the oxidant copper phenanthroline at either room temperature (20°C) or on ice. As shown in Fig. 5A, disulfide-bonded dimer was formed to similar extents at both ambient and low temperatures, strongly suggesting that the cross-link was between TatC protomers within a TatBC complex.

Figure 6 summarizes the results we obtained for disulfide cross-linking, performed at room temperature, of each of the 36 cysteine-containing TatC variants with substitutions in transmembrane regions. It is clear (Fig. 6A) that none of the cysteine substitutions in transmembrane helix one were in close enough proximity to similar residues in other TatC molecules to form a disulfide cross-link. By contrast, cross-linking analysis of cysteine residues in TatC transmembrane helix two (Fig. 6B) showed two positions where the introduction of cysteine residues and exposure to oxidizing agent resulted in the formation of a disulfide-bonded dimer. A TatC variant harboring a cysteine substitution at residue 82 produced a low level of cross-linked dimer, while a substitution at position 86 gave an almost complete cross-link to dimer form. Plotting the positions of those residues on a helical wheel projection of this part of the protein, depicted in Fig. 7A, shows that both of these residues would fall on the same helical face, indicating that there is facial specificity for the self-interaction of this portion of transmembrane helix two. None of these cross-links were observed when oxidation was carried out on ice (not shown), which suggests that interactions are probably between TatC proteins located in separate TatBC complexes.

The results of disulfide cross-linking experiments of TatC variants expressing single cysteine substitutions in transmembrane helix three are shown in Fig. 6C. The first three residues that we tested (positions 124 to 126) did not show any cross-linking, while the latter three residues (127 to 129) all showed some level of dimer formation in the presence of oxidant. Reasonably strong dimer bands were observed for TatC F127C and V129C, and a weaker cross-link was observed for V128C. When these residues are plotted onto a helical wheel representation, shown in Fig. 7B, there is no obvious facial specificity to the interaction. Moreover, the fact that the first three residues that we tested failed to self-cross-link suggests that these helices in the TatC interface are tilted relative to each other, assuming that this portion of the protein is helical. Again, all cross-links were strongly influenced by mobility because they were lost when oxidation was carried out at lower temperatures (not shown), and we therefore conclude that they are probably formed between different complexes.

A surprisingly large number of self-cross-links were also observed when TatC cysteine variants in transmembrane helix four were exposed to oxidant (Fig. 6D). A rather strong cross-link was seen for the cysteine substitution at residue 169, and a slightly weaker one was seen at G166, both of which would cluster on one face of a α-helix (Fig. 7C). Cross-links were also observed for cysteine substitutions at residues 167 and 171, which would also cluster together on one face of a putative α-helix (Fig. 7C). No cross-links were detected for substitutions at positions 168 and 170, and all observed cross-links were again lost when samples were oxidized on ice (not shown), which indicates that they are formed between complexes. The positions of the cross-linking residues on a helical wheel representation (Fig. 7C) are consistent with two, almost completely opposite, faces of self-interaction for transmembrane helix four.

Analysis of patterns of disulfide cross-linking for TatC cysteine variants in transmembrane helix five are shown in Fig. 6E. Again, an unexpectedly large number of cross-links was

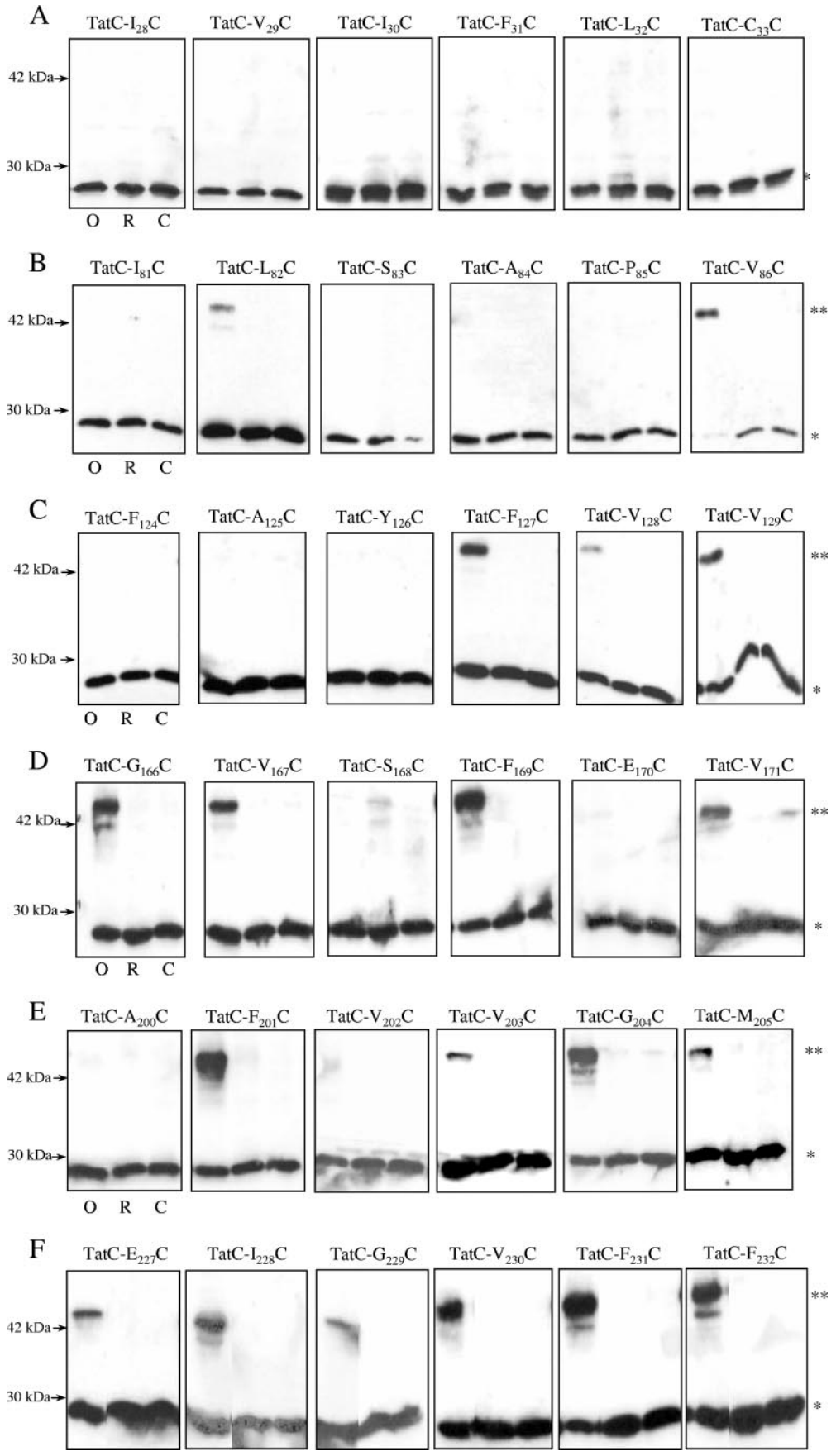

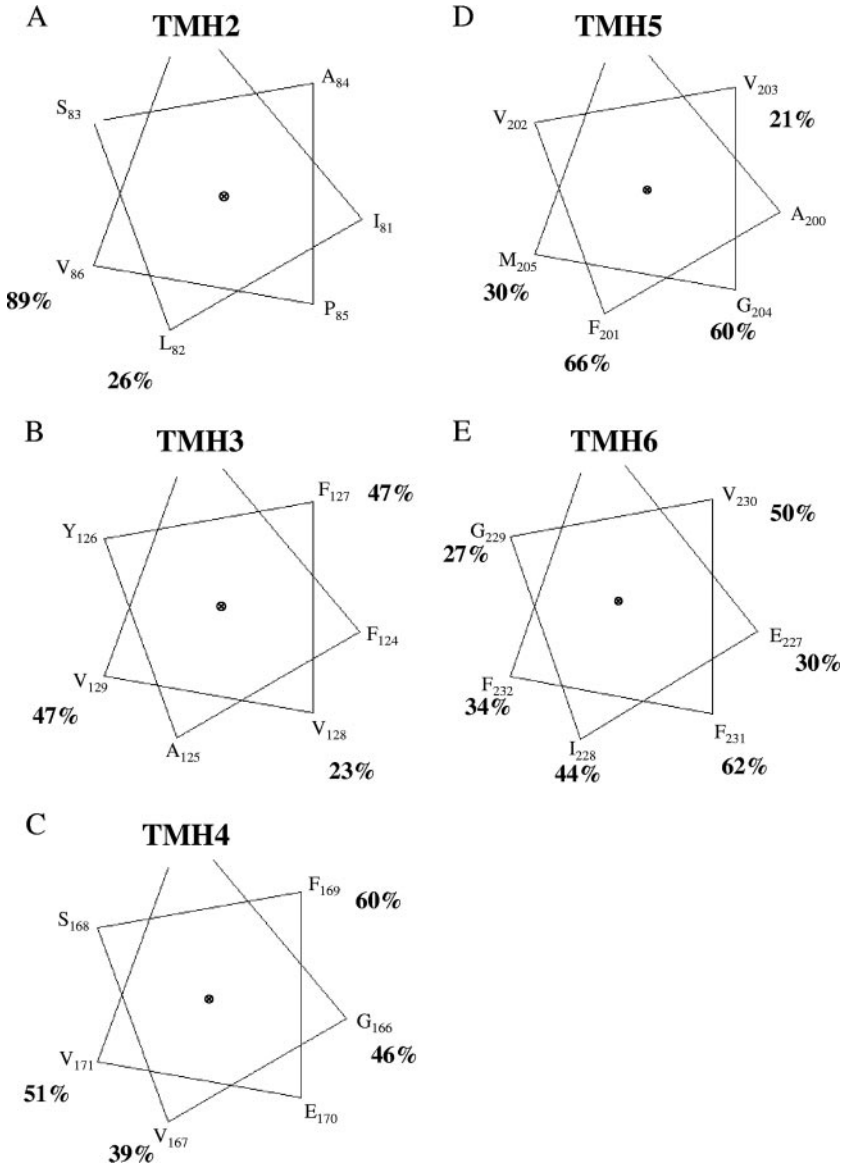

FIG. 7. Helical wheel projections of portions of TatC transmembrane helix two (TMH2) to transmembrane helix six (TMH6) that were analyzed by disulfide cross-linking. The percentage next to each residue is the percentage of cross-linked dimer (expressed as a percentage of monomer plus dimer) formed after oxidation at room temperature for 1 h.

detected when samples were oxidized at room temperature, and again, none of these were observed when samples were oxidized at 0°C, suggesting that they are primarily between different TatBC complexes. TatC F201C and G204C gave strong cross-linked dimer bands under oxidizing conditions, whereas TatC V203C and M205C gave much weaker cross-linked dimer bands. TatC A200C and V202C did not form cross-linked dimers. A plot of these residues on a helical wheel

FIG. 6. Immunoblot analysis of cross-linked *E. coli* TatC proteins containing cysteine substitutions in each transmembrane helix. Membrane samples were prepared from the Δ*tatABCD* Δ*tatE pcnB* strain, DADE-P, coexpressing single cysteine-substituted TatC variants together with TatA and TatB from pUNITATCC4. Samples (100 μg membrane protein) were subjected to either oxidizing conditions (O; shown in the leftmost lane for each sample) or reducing conditions (R; middle lane for each sample) or incubated with buffer alone (C; rightmost lane for each sample) each at room temperature as described in Materials and Methods. Samples (10 μg membrane protein) were resolved by SDS-PAGE (12.5% acrylamide), and TatC proteins were visualized by immunoblotting with anti-TatC antisera. The position of the cysteine substitution is shown above each panel. The positions of TatC monomer (*) and dimer (**) forms are indicated. (A) Substitutions in transmembrane helix one; (B) substitutions in transmembrane helix two; (C) substitutions in transmembrane helix three; (D) substitutions in transmembrane helix four; (E) substitutions in transmembrane helix five; (F) substitutions in transmembrane helix six.

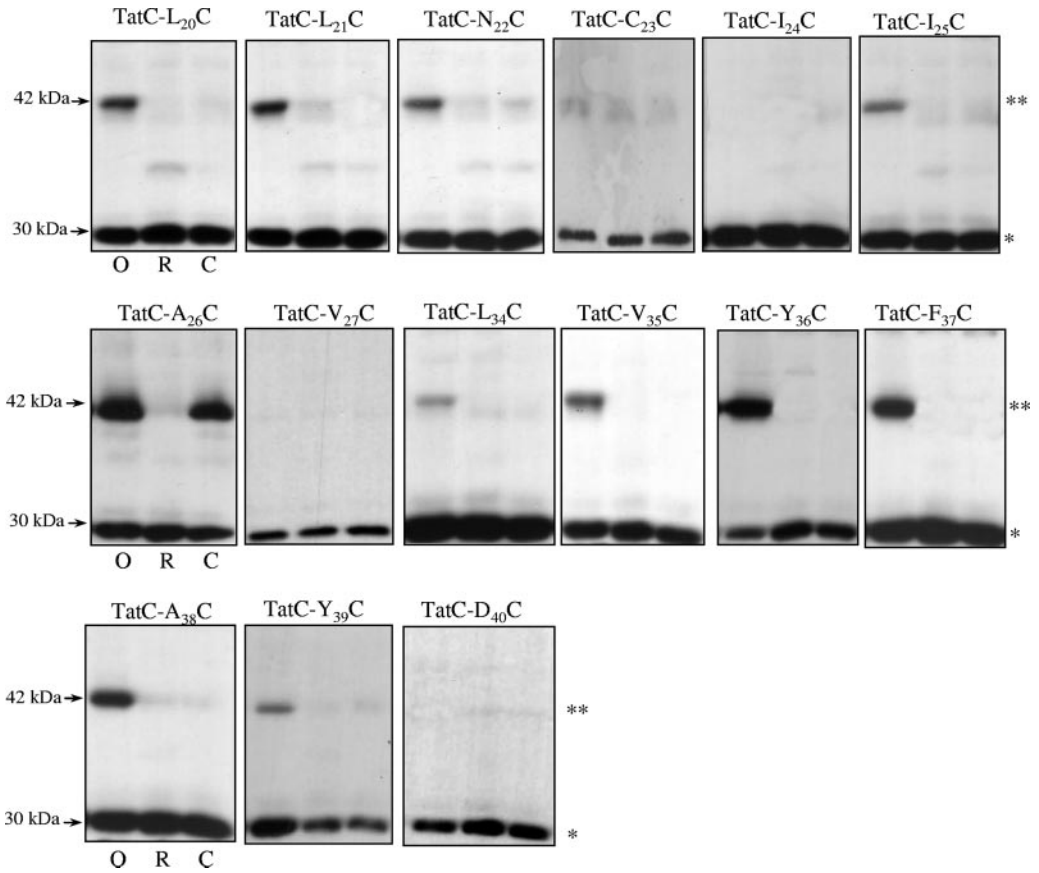

FIG. 8. Immunoblot analysis of cross-linked *E. coli* TatC proteins containing further cysteine substitutions in transmembrane helix one. Membrane samples were prepared from the Δ*tatABCD* Δ*tatE pcnB* strain, DADE-P, coexpressing single cysteine-substituted TatC variants together with TatA and TatB from pUNITATCC4. Samples (100 μg membrane protein) were subjected to either oxidizing conditions (O; shown in the leftmost lane for each sample) or reducing conditions (R; middle lane for each sample) or incubated with buffer alone (C; rightmost lane for each sample), each at room temperature. Samples (10 μg membrane protein) were resolved by SDS-PAGE (12.5% acrylamide), and TatC proteins were visualized by immunoblotting with anti-TatC antisera. The position of the cysteine substitution is shown above each panel. The positions of TatC monomer (*) and dimer (**) forms are indicated.

projection (Fig. 7D) again shows at least two faces of self-interaction—a strongly interacting face comprising F201 and G204, possibly extending as far as M205, and a weaker face comprising V203.

Figures 6F and 7E summarize the cross-linking results we observed when TatC variants with cysteine substitutions in transmembrane helix six were incubated at room temperature in the presence of oxidant. Surprisingly, every one of the six consecutive cysteine substitutions that we tested showed formation of a significant level of self-cross-linked dimer under oxidizing conditions. These observations suggest that this part of the protein in particular must be highly mobile to allow each of these residues into close proximity with their counterparts in other TatC proteins. Again no cross-links were seen after oxidation on ice (not shown), emphasizing that mobility is essential for cross-link formation and suggesting that the interactions we detect are likely to be between different TatC-containing complexes.

Cysteine scanning mutagenesis and disulfide cross-linking analysis of the remaining residues in TatC transmembrane helix one. Our cysteine cross-linking analysis showed that each of the putative transmembrane helices of TatC exhibited self-interaction with the exception of the first transmembrane helix. These observations would be consistent with the possibility that this part of TatC is tightly buried within the TatC monomer, thus preventing self-contact. In order to test this hypothesis, we constructed a further 15 individual cysteine substitutions in transmembrane helix one, covering residues L20 to V27 and L34 to D40, respectively (Fig. 1).

As shown in Fig. 2C, each of these substitutions gave rise to a TatC protein that was competent to support protein transport. Substitutions in the first part of the helix (positions 20 to 23) gave TatC proteins that were almost as active as the wild type. A previous study showed that L20A substitution of TatC was also active, although a deletion of residues 20 through 22 did inactivate the protein (2). Substitutions further along the helix, in particular the alanine residues at positions 26 and 38, had quite a marked effect on Tat-dependent transport, but even the most severely affected mutations still supported around 25% of the wild-type Tat activity.

The results of disulfide cross-linking analysis, undertaken at room temperature, on these additional cysteine-substituted TatC proteins are shown in Fig. 8. Residues V27C and L34C, which are immediately adjacent to the six non-cross-linking

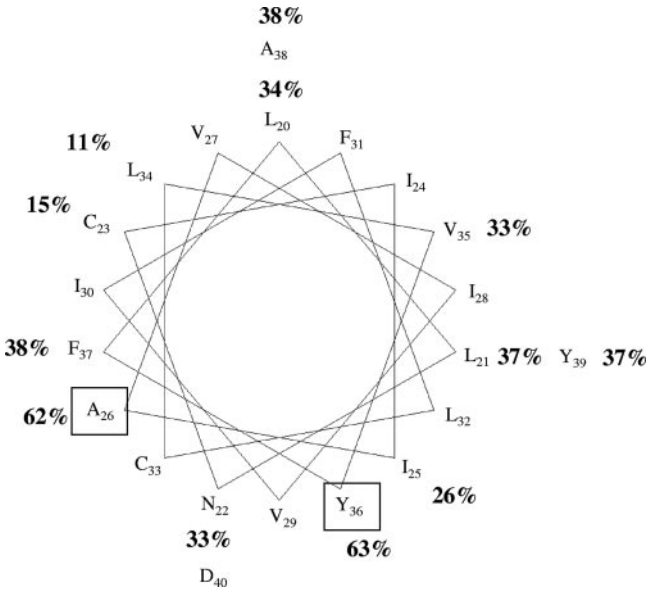

FIG. 9. Helical wheel projection for the entire TatC transmembrane helix one. For those residues that show cross-linking, the percentage of cross-linked dimer (expressed as a percentage of monomer plus dimer) formed after oxidation at room temperature for 1 h is indicated. Residues A26 and Y36 are shown boxed.

residues of TatC that we tested above, similarly show no or very little self-cross-linking. However, many of the substitutions towards the ends of the helix in either direction show significant disulfide bond formation upon oxidation. The ends of helices in general have greater mobility, and similar nonperiodic cross-linking was also seen with cysteine substitutions at either end of the TatB transmembrane helix (23). Residue A26C also formed a disulfide-bonded dimer prior to the addition of catalyst, suggesting that this residue may be uniquely exposed to an oxidizing environment in the membrane. These observations are therefore not consistent with the idea that transmembrane helix one is buried within the TatC monomer.

When the cross-linking analysis was repeated at 0°C, most of the cross-links were lost with the exception of homodimeric cross-linking of residues A26C and Y36C (shown in Fig. 5B and C) which still gave significant dimer formation at low temperatures. Therefore, we conclude that most of the observed cross-links are probably between TatC proteins located within different TatBC complexes with the exception of the A26C and Y36C variants which are likely to be cross-links within a single complex. A helical wheel projection of the entire transmembrane helix one is shown in Fig. 9, with the percentage of dimer formation (after oxidation at room temperature) indicated for those residues that show disulfide cross-linking. Residues A26 and Y36 (Fig. 9) do not fall on the same face of a regular α-helix, which suggests either that this helix may be twisted or that this helix can self-interact with more than one TatC partner.

DISCUSSION

In this study we have constructed a series of cysteine substitutions in the TatC protein to probe the topology and self-interaction of TatC. In total, we substituted 57 individual residues, i.e., some 22% of the protein, for cysteine. None of the substitutions that we constructed gave rise to an inactive TatC protein, indicating that in general, mutation of the protein is well tolerated. This is consistent with previous studies that targeted highly conserved residues of TatC, where very few essential residues were identified (2, 8).

We used a subset of these cysteine variants for topological labeling studies on the protein. Previous reports used fusion approaches to assess the cellular locations of residues within and between each putative transmembrane helix (4, 18, 21). These, with the exception of fusions at the extreme termini, necessarily disrupt the function of the protein. In this work, labeling experiments were carried out on TatC proteins that were mostly fully active, giving results that were consistent with the presence of six transmembrane spans in the protein. Since this technique is noninvasive, it opens up the possibility of probing topological rearrangements in TatC that might accompany protein transport.

Cross-linking experiments on TatC proteins harboring single cysteine substitutions in the likely membrane-spanning regions showed that each individual transmembrane helix of TatC was in close proximity with the same helix from a neighboring molecule. Moreover, several of these helices appeared to self-cross-link through multiple faces. Further analysis showed that almost all of the cross-links were abolished when membrane protein mobility was reduced by incubation on ice, pointing to the likelihood that the interactions we observed were between TatC proteins that were in different complexes. This would support the conclusion from TatB disulfide cross-linking studies (23) that TatC is located on the outside of the TatBC complex. An alternative possibility is that there are multiple conformers of TatC within the TatBC complex and that interconversion of these conformers is prevented at low temperature, resulting in loss of cross-linking. We think this idea is less likely because cross-linking of three of the TatC variants, TatC A26C, Y36C and G144C, was not affected by incubation on ice. Moreover, it would be unexpected to detect so many specific interactions in other conformational states and almost none in the lowest energy state. Therefore, we propose that these three residues represent points at which one or more TatC protomers form sites of close contact, supporting the notion that TatC within the TatBC complex forms a homomultimer.

ACKNOWLEDGMENTS

We thank Frank Sargent for helpful discussions and George Georgiou for providing us with strain LM107.

This work was supported by a John Innes Foundation Studentship (to C.P.), the Medical Research Council via a Senior Non-Clinical Fellowship award to T.P., by the Wellcome Trust through grant number 061780, and by the BBSRC through grant 43/P16795 and a grant-in-aid to the John Innes Centre.

REFERENCES

1. **Alami, M., I. Luke, S. Deitermann, G. Eisner, H. G. Koch, J. Brunner, and M. Müller.** 2003. Differential interactions between a twin-arginine signal peptide and its translocase in *Escherichia coli*. Mol. Cell **12:**937–946.
2. **Allen, S. C., C. M. Barrett, N. Ray, and C. Robinson.** 2002. Essential cytoplasmic domains in the *Escherichia coli* TatC protein. J. Biol. Chem. **277:**10362–10366.
3. **Banerjee, S., and D. G. Fraenkel.** 1972. Glucose-6-phosphate dehydrogenase from *Escherichia coli* and from a "high-level" mutant. J. Bacteriol. **110:**155–160.
4. **Behrendt, J., K. Standar, U. Lindenstrauss, and T. Brüser.** 2004. Topolog-

ical studies on the twin-arginine translocase component TatC. FEMS Microbiol. Lett. **234:**303–308.
5. **Berks, B. C., T. Palmer, and F. Sargent.** 2003. The Tat protein translocation pathway and its role in microbial physiology. Adv. Microb. Physiol. **47:**187–254.
6. **Bogsch, E., F. Sargent, N. R. Stanley, B. C. Berks, C. Robinson, and T. Palmer.** 1998. An essential component of a novel bacterial protein export system with homologues in plastids and mitochondria. J. Biol. Chem. **273:** 18003–18006.
7. **Bolhuis, A., J. E. Mathers, J. D. Thomas, C. M. Barrett, and C. Robinson.** 2001. TatB and TatC form a functional and structural unit of the twin-arginine translocase from *Escherichia coli*. J. Biol. Chem. **276:**20213–20219.
8. **Buchanan, G., E. de Leeuw, N. R. Stanley, M. Wexler, B. C. Berks, F. Sargent, and T. Palmer.** 2002. Functional complexity of the twin-arginine translocase TatC component revealed by site-directed mutagenesis. Mol. Microbiol. **43:**1457–1470.
9. **Casadaban, M. J., and S. N. Cohen.** 1979. Lactose genes fused to exogenous promoters in one step using a Mu-lac bacteriophage: *in vivo* probe for transcriptional control sequences. Proc. Natl. Acad. Sci. USA **76:**4530–4533.
10. **Cline, K., and H. Mori.** 2001. Thylakoid ΔpH-dependent precursor proteins bind to a cpTatC-Hcf106 complex before Tha4-dependent transport. J. Cell Biol. **154:**719–729.
11. **Cohen, G. N., and H. W. Rickenberg.** 1956. Concentration specifique reversible des amino acids chez *Escherichia coli*. Ann. Inst. Pasteur (Paris) **91:**693–720.
12. **de Leeuw, E., I. Porcelli, F. Sargent, T. Palmer, and B. C. Berks.** 2001. Membrane interactions and self-association of the TatA and TatB components of the twin-arginine translocation pathway. FEBS Lett. **506:**143–148.
13. **de Leeuw, E., T. Granjon, I. Porcelli, M. Alami, S. B. Carr, M. Müller, F. Sargent, T. Palmer, and B. C. Berks.** 2002. Oligomeric properties and signal peptide binding by *Escherichia coli* Tat protein transport complexes. J. Mol. Biol. **322:**1135–1146.
14. **De Mendoza, D., and J. E. Cronan, Jr.** 1983. Thermal regulation of membrane lipid fluidity in bacteria. Trends Biochem. Sci. **8:**49–52.
15. **Drew, D., D. Sjöstrand, J. Nilsson, T. Urbig, C. N. Chin, J. W. de Gier, and G. von Heijne.** 2002. Rapid topology mapping of *Escherichia coli* inner-membrane proteins by prediction and PhoA/GFP fusion analysis. Proc. Natl. Acad. Sci. USA **99:**2690–2695.
16. **Gerard, F., and K. Cline.** 2006. Efficient twin arginine translocation (Tat) pathway transport of a precursor protein covalently anchored to its initial cpTatC binding site. J. Biol. Chem. **281:**6130–6135.
17. **Gohlke, U., L. Pullan, C. A. McDevitt, I. Porcelli, E. de Leeuw, T. Palmer, H. Saibil, and B. C. Berks.** 2005. The TatA component of the twin-arginine protein transport system forms channel complexes of variable diameter. Proc. Natl. Acad. Sci. USA **102:**10482–10486.
18. **Gouffi, K., C.-L. Santini, and L.-F. Wu.** 2002. Topology determination and functional analysis of the *Escherichia coli* TatC protein. FEBS Lett. **525:**65–70.
19. **Iwaki, S., N. Tamura, T. Kimura-Someya, S. Nada, and A. Yamaguchi.** 2000. Cysteine-scanning mutagenesis of transmembrane segments 4 and 5 of the *Tn*10-encoded metal-tetracycline/H+ antiporter reveals a permeability barrier in the middle of a transmembrane water-filled channel. J. Biol. Chem. **275:**22704–22712.
20. **Jack, R. L., F. Sargent, B. C. Berks, G. Sawers, and T. Palmer.** 2001. Constitutive expression of *Escherichia coli tat* genes indicates an important role for the twin-arginine translocase during aerobic and anaerobic growth. J. Bacteriol. **183:**1801–1804.
21. **Ki, J. J., Y. Kawarasaki, J. Gam, B. R. Harvey, B. L. Iverson, and G. Georgiou.** 2004. A periplasmic fluorescent reporter protein and its application in high-throughput membrane protein topology analysis. J. Mol. Biol. **341:**901–909.
22. **Laemmli, U. K.** 1970. Cleavage of structural proteins during the assembly of the head of bacteriophage T4. Nature **277:**680–685.
23. **Lee, P. A., G. Orriss, G. Buchanan, N. P. Greene, P. J. Bond, C. Punginelli, R. L. Jack, M. S. P. Sansom, B. C. Berks, and T. Palmer.** 2006. Cysteine-scanning mutagenesis and disulfide mapping studies of the conserved domain of the twin-arginine translocase TatB component. J. Biol. Chem. **281:** 34072–34085.
24. **Liu, J. D., and J. S. Parkinson.** 1989. Genetics and sequence analysis of the *pcnB* locus, an *Escherichia coli* gene involved in plasmid copy number control. J. Bacteriol. **171:**1254–1261.
25. **Lowry, O. H., N. J. Rosebrough, A. L. Farr, and R. J. Randall.** 1951. Protein measurements with the Folin phenol reagent. J. Biol. Chem. **193:**265–275.
26. **Mansilla, M. C., L. E. Cybulski, D. Albanesi, and D. de Mendoza.** 2004. Control of membrane lipid fluidity by molecular thermosensors. J. Bacteriol. **186:**6681–6688.
27. **Manting, E. H., and A. J. Driessen.** 2000. *Escherichia coli* translocase: the unravelling of a molecular machine. Mol. Microbiol. **37:**226–238.
28. **Masip, L., J. L. Pan, S. Haldar, J. E. Penner-Hahn, M. P. DeLisa, G. Georgiou, J. C. Bardwell, and J. F. Collet.** 2004. An engineered pathway for the formation of protein disulfide bonds. Science **303:**1185–1189.
29. **McDevitt, C. A., M. G. Hicks, T. Palmer, and B. C. Berks.** 2005. Characterisation of Tat protein transport complexes carrying inactivating mutations. Biochem. Biophys. Res. Commun. **329:**693–698.
30. **McDevitt, C. A., G. Buchanan, F. Sargent, T. Palmer, and B. C. Berks.** 2006. Subunit composition and *in vivo* substrate binding characteristics of *Escherichia coli* Tat protein complexes expressed at native levels. FEBS J. **273:** 5656–5668.
31. **Mori, H., and K. Cline.** 2001. Post-translational protein translocation into thylakoids by the Sec and ΔpH-dependent pathways. Biochim. Biophys. Acta **1541:**80–90.
32. **Nagy, J. K., F. W. Lau, J. U. Bowie, and C. R. Sanders.** 2000. Mapping the oligomeric interface of diacylglycerol kinase by engineered thiol cross-linking: homologous sites in the transmembrane domain. Biochemistry **39:**4154–4164.
33. **Oates, J., J. Mathers, D. Mangels, W. Kuhlbrandt, C. Robinson, and K. Model.** 2003. Consensus structural features of purified bacterial TatABC complexes. J. Mol. Biol. **330:**277–286.
34. **Oates, J., C. M. Barrett, J. P. Barnett, K. G. Byrne, A. Bolhuis, and C. Robinson.** 2005. The *Escherichia coli* twin-arginine translocation apparatus incorporates a distinct form of TatABC complex, spectrum of modular TatA complexes and minor TatAB complex. J. Mol. Biol. **346:**295–305.
35. **Porcelli, I., E. de Leeuw, R. Wallis, E. van den Brink-van der Laan, B. de Kruijff, B. A. Wallace, T. Palmer, and B. C. Berks.** 2002. Characterisation and membrane assembly of the TatA component of the *Escherichia coli* twin-arginine protein transport system. Biochemistry **41:**13690–13697.
36. **Sambrook, J., E. F. Fritsch, and T. Maniatis.** 1989. Molecular cloning: a laboratory manual, 2nd ed. Cold Spring Harbor Laboratory Press, Cold Spring Harbor, NY.
37. **Sargent, F., E. Bogsch, N. R. Stanley, M. Wexler, C. Robinson, B. C. Berks, and T. Palmer.** 1998. Overlapping functions of components of a bacterial Sec-independent protein export pathway. EMBO J. **17:**3640–3650.
38. **Sargent, F., N. R. Stanley, B. C. Berks, and T. Palmer.** 1999. Sec-independent protein translocation in *Escherichia coli*: a distinct and pivotal role for the TatB protein. J. Biol. Chem. **274:**36073–36083.
39. **Sargent, F., U. Gohlke, E. de Leeuw, N. R. Stanley, T. Palmer, H. R. Saibil, and B. C. Berks.** 2001. Purified components of the *Escherichia coli* Tat protein transport system form a double-layered ring structure. Eur. J. Biochem. **268:**3361–3367.
40. **Silvestro, A., J. Pommier, and G. Giordano.** 1988. The inducible trimethylamine-*N*-oxide reductase of *Escherichia coli* K12: biochemical and immunological studies. Biochim. Biophys. Acta **954:**1–13.
41. **Stanley, N. R., T. Palmer, and B. C. Berks.** 2000. The twin arginine consensus motif of Tat signal peptides is involved in Sec-independent protein targeting in *Escherichia coli*. J. Biol. Chem. **275:**11591–11596.
42. **Tang, X. B., J. Fujinaga, R. Kopito, and J. R. Casey.** 1998. Topology of the region surrounding Glu681 of human AE1 protein, the erythrocyte anion exchanger. J. Biol. Chem. **273:**22545–22553.
43. **Towbin, H., T. Staehelin, and J. Gordon.** 1979. Electrophoretic transfer of proteins from polyacrylamide gels to nitrocellulose sheets: procedure and some applications. Proc. Natl. Acad. Sci. USA **76:**4350–4354.
44. **Weiner, J. H., P. T. Bilous, G. M. Shaw, S. P. Lubitz, L. Frost, G. H. Thomas, J. A. Cole, and R. J. Turner.** 1998. A novel and ubiquitous system for membrane targeting and secretion of cofactor-containing proteins. Cell **93:** 93–101.